coatings

MDPI

Communication

Reconstructed Cd(0001) Surface Induced by Adsorption of Triphenyl Bismuth

Mengmeng Bai, Zuo Li, Mingxia Shi, Minlong Tao, Kai Sun, Xiaotian Yang, Yufeng Zhang and Junzhong Wang *

School of Physical Science and Technology, Southwest University, Chongqing 400715, China
* Correspondence: jzwangcn@swu.edu.cn

Abstract: Largish molecules on metal surfaces may act as not only the building blocks of 2D self-assemblies, but also as the template to reshape the metal surfaces. Here, we report the molecular adsorption-induced formation of the periodic nanostripe arrays of substrate atoms through long-range mass transport. When adsorbed on the close-packed Cd(0001) surface, the triphenyl bismuth (TPB) molecules form a 2D self-assembly with $4 \times \sqrt{13}$ reconstruction. Simultaneously, periodic nanostripe arrays of Cd atoms appear on the substrate terraces. High-resolution scanning tunneling microscopy (STM) images indicate that the Cd nanostrips are built from the parallel segments of Cd atomic chains with 2×2 reconstruction. In the mixed phase, the Cd atomic chains exhibit only high-order commensuration when situated between two molecular domains. The massive structural rearrangement of the Cd(0001) surface can be attributed to a strong molecule–substrate interaction.

Keywords: triphenyl bismuth; Cd(0001) surface; STM; nanostripe; atomic chains

Citation: Bai, M.; Li, Z.; Shi, M.; Tao, M.; Sun, K.; Yang, X.; Zhang, Y.; Wang, J. Reconstructed Cd(0001) Surface Induced by Adsorption of Triphenyl Bismuth. *Coatings* **2023**, *13*, 394. https://doi.org/10.3390/coatings13020394

Academic Editor: Cristian Vacacela Gomez

Received: 21 January 2023
Revised: 1 February 2023
Accepted: 4 February 2023
Published: 8 February 2023

1. Introduction

The interaction between large organic molecules and metal surfaces has recently been the focus of molecular self-assembly and nanostructure fabrications due to the important applications in organic electronics and nanodevices [1]. In general, the structures of molecular self-assemblies on surfaces are controlled by the delicate balance between the intermolecular and molecule–substrate interactions [2]. However, when largish molecules are deposited on metal surfaces, the molecule–substrate interactions may be rather complex such that the molecules are not only the building blocks of a self-assembled monolayer, but also the templates to reshape the metal substrates [3–27]. In other words, the metal surfaces do not always behave as static substrates but may rearrange dramatically to accommodate the largish molecules.

The first molecule-induced substrate reconstruction was observed at the interfaces between fullerene and metal surfaces [5–9]. When adsorbed on Au(110) surfaces, fullerene molecules can induce the significant mass transport of Au adatoms to form a 1×5 reconstruction [5]. The fullerene molecules adsorbed on Pd(110) lead to the formation of Pd islands due to the presence of mobile Pd adatoms [6]. The Lander molecules on Cu(110) can act as a molecular template to reshape the substrate step edges into metallic nanostructures [10–12]. The HtBDC molecules deposited on the Cu(110) surface also result in the formation of characteristic trenches, in which Cu atoms are dug out of the substrate [13]. Moreover, the periodic nanostrips of Cu atoms appeared on a Cu(110) surface after depositing one monolayer of perylene molecules [14]. Recently, Tseng et al. demonstrated that a strong charge-transfer between Cu(100) and tetracyano-p-quinodimethane [TCNQ] leads to the substantial structural rearrangements at both sides of metal-organic interfaces [15].

It is noteworthy that nearly all the metal substrates mentioned above are limited to the open surfaces, such as fcc(110) or fcc(100), which display an intrinsic instability. It remains unclear whether the close-packing metal surfaces, such as fcc(111) or hcp(0001), can be reconstructed by large molecules [28–30]. On the other hand, the modified substrate

regions are localized underneath or adjacent to the molecular domains such that long-range mass transports of substrate atoms are rarely observed.

Triphenyl bismuth (TPB) is a typical organometallic compound with three-fold symmetry [31]. The density function theory (DFT) calculation suggested that the Kagome lattice of TPB is a 2D organic topological insulator with quantum edge states and a Dirac cone gap of ~43 meV [32]. Recently, the topological ordering in 2D materials has received a widespread interest in order to find low-energy materials. The robust conducting edge states are protected from the elastic backscattering and electron localizations and have potential applications in the quantum information and spintronics. Compared with the inorganic topological insulators, the organic topological insulators have the advantages of low costs, an easy fabrication, and mechanical flexibility. Recent transport measurements indicated that superconductivity occurs in the K-doped TPB with a critical temperature of 3.5~7.2 K [33,34]. In this work, we have studied the 2D self-assembly of TPB molecules on the close-packing Cd(0001) surface and the molecule-induced rearrangement of the Cd substrate. It is observed that, in the submonolayer regime, the TPB molecules form a 2D self-assembled structure with oblique lattices. Simultaneously, the adsorption-induced substrate reconstruction takes place in the form of periodic nanostrips of Cd atoms. Most importantly, the transport distances of Cd atoms can reach to several hundred nanometers, which was not observed in the previous experiments. To the best of our knowledge, this is the first observation of the structural rearrangement of a close-packed surface induced by the adsorption of largish organic molecules.

2. Experimental Method

The experiments were performed in an ultrahigh vacuum low-temperature STM (Unisoku USM1500) with a base pressure of ~1.2×10^{-10} Torr. The Si(111)-7 × 7 surface was prepared by overnight degassing at ~600 K and, subsequently, flashing to 1500 K. Cd atoms with a purity of 99.998% were thermally evaporated from a quartz crucible onto the Si(111)-7 × 7 surface. Flat and smooth Cd(0001) thin films were obtained by depositing 10~15 monolayers (ML) of Cd atoms on a Si(111)-7 × 7 surface, Figure 1b. The terraces of Cd thin films exhibit wavy step edges. The measured step height is 2.8 ± 0.1 Å, consistent with the interplanar distance of crystalline Cd(0001) films. The Cd(0001) thin films reveal hexagonal lattices (c_0 = 3.0 Å), as indicated by the parallelogram unit-cell in Figure 1c. TPB molecules (Adamas, 99%) were thermally sublimated from a boron nitride crucible heated to ~360 K. The deposition rate is around 0.2 ML per minute with the Cd(0001) substrate kept at a low temperature (90 K). After TPB deposition, the sample was swiftly transferred to the low-temperature STM chamber. Before measurement, the STM tip was treated by electron-beam bombardment to remove of the contamination and oxidation. All STM images were recorded in the constant current mode at a low temperature of 77 K.

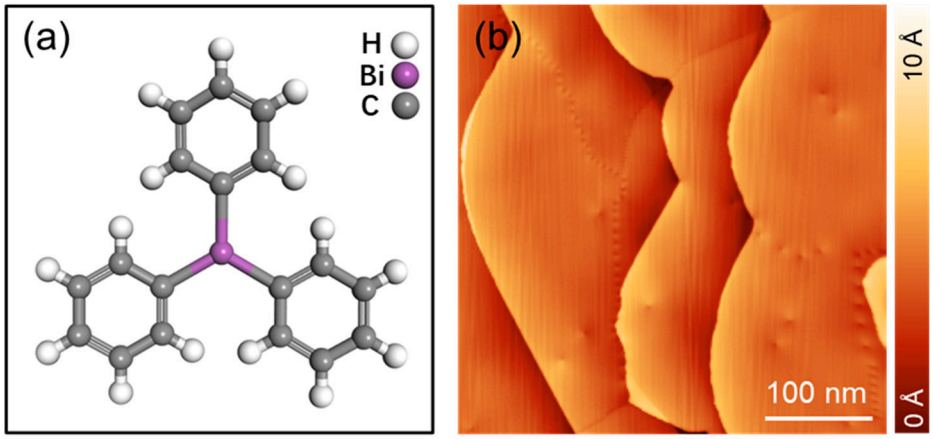

Figure 1. *Cont.*

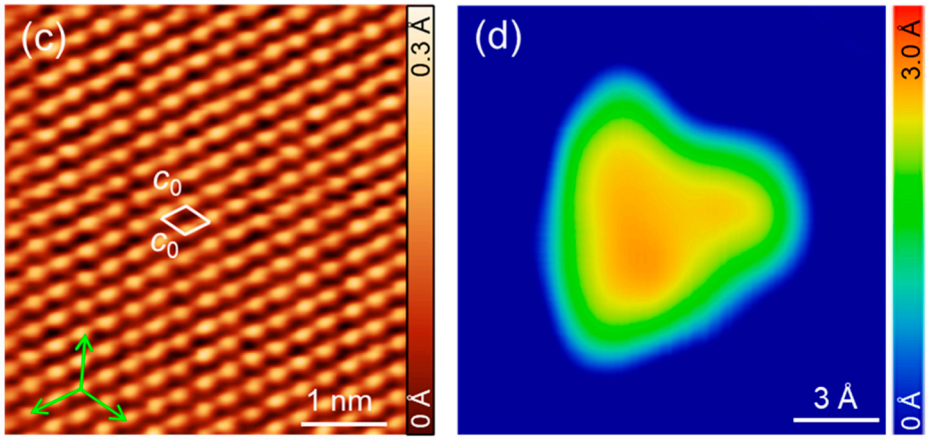

Figure 1. Isolated TPB molecule adsorbed on Cd(0001). (**a**) Chemical structure of TPB molecule. (**b**) Morphology of the Cd(0001) thin films grown on a Si(111)-7 × 7, 3.0 V, 20 pA. (**c**) Atomic-resolution STM image showing the hexagonal lattice of the Cd(0001) thin film, 0.06 V, 20 pA. (**d**) STM image of an isolated TPB molecule adsorbed on Cd(0001), revealing a three-lobe motif, 0.9 V, 20 pA.

3. Results and Discussion

We firstly deposited a small amount of TPB molecules on a Cd(0001) surface, which was kept at a low temperature (90 K). It is observed from Figure 1d that the isolated TPB molecule manifests as a three-lobe motif. The three lobes reveal a different brightness with a height difference of ~0.1 Å, which may arise from the molecular conformational change or tilted orientation of a TPB on Cd(0001).

When the coverage is increased to ~0.3 ML, the TPB molecules form a 2D self-assembled structure (Figure 2a). As revealed by the cross-sectional profile line (Figure 2b), the TPB layer has an apparent height of 1.2 Å at the bias voltage of 2.5 V. A few bright protrusions can be observed on top of the TPB layer, corresponding to the TPB molecules of the second layer. From the close-up view in Figure 2c, the self-assembled domain shows an oblique lattice with $a = 10.7 \pm 0.2$ Å, $b = 12.5 \pm 0.2$ Å, $\theta = 48 \pm 5°$ corresponding to the $4 \times \sqrt{13}$ reconstruction. From the high-resolution image shown in Figure 2d, it is found that the individual TPB molecule appears as a cloverleaf pattern with one lobe higher than the other two, unlike the isolated TPB molecule (Figure 1d). We speculate that molecular conformational changes take place in the self-assembled monolayer. Driven by the intermolecular interaction and molecule–substrate interactions, one benzene ring of TPB is twisted out of the molecular plane such that one benzene ring is higher than the other twos, as occurred in the TPB crystals [26].

Besides the 2D self-assembled domains of TPB, a mixed phase made of the TPB molecular row and nanostrips of the Cd atoms has been found on the terraces of Cd(0001). In the upper-right part of a TPB domain, there are some parallel trenches with different lengths (Figure 3a). From the close-up view (Figure 3b), it is observed that the individual trenches (nanostrips) are composed of parallel segments of Cd atomic chains, which are aligned at two different directions. The trenches are separated by 2D self-assembled TPB domains, which have a width of three or four molecular rows. The measured lattice constants of the molecular rows are the same as those in the 2D self-assembled domains shown in Figure 2.

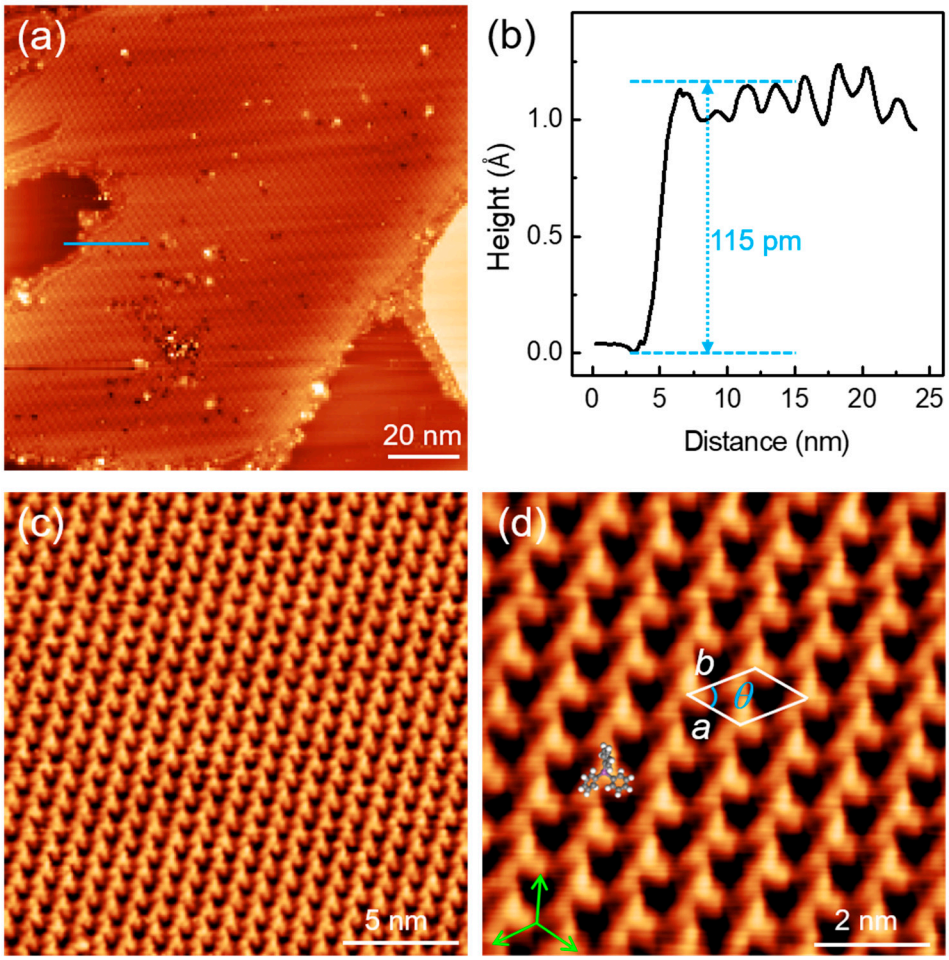

Figure 2. 2D self-assembly of TPB molecules on Cd(0001). (**a**) A monolayer island of self-assembled TPB formed on Cd(0001), 2.5 V, 30 pA. (**b**) Cross-sectional profile line taken along the blue line in (**a**), showing the apparent height of TPB layer. (**c**,**d**) Close-up views of the 2D self-assembly of TPB, showing an oblique lattice with $4 \times \sqrt{13}$ reconstruction, 0.1 V, 20 pA.

Figure 3c,d show a typical trench structure confined by two TPB domains. The height difference between the molecular layer and Cd atomic chains is ~28 pm (Figure 3e), which is much smaller than the height difference between the TPB layer and bare Cd substrate. It means that the Cd atomic chains are not the reconstruction of the Cd(0001) surface layer, but the nanostructures made of migrated Cd atoms. We noticed that the Cd chains and TPB molecules exhibit a strong bias-dependent heights. As shown in Figure S1, the apparent heights of Cd chains and TPB molecules reach to 2.0 ± 0.1 Å and 4.0 ± 0.1 Å, respectively. The mass transport of Cd atoms takes place from the substrate areas beneath the TPB layer or from the step edges of Cd(0001) to the trench regions. When the bias voltage is reduced to 0.03 V, the trench structure exhibits atomic-resolution protrusions (Figure 3f). The atomic chains show an oblique lattice with $c_1 = 6.9 \pm 0.2$ Å, $c_2 = 6.0 \pm 0.2$Å, $\beta = 60° \pm 5°$. It can be found that $c_2 = 2c_0$ and $3c_1 \approx 7c_0$, indicating the high-order commensuration along the c_2 direction. Thus, each protrusion inside the trenches can be assigned as a Cd dimer.

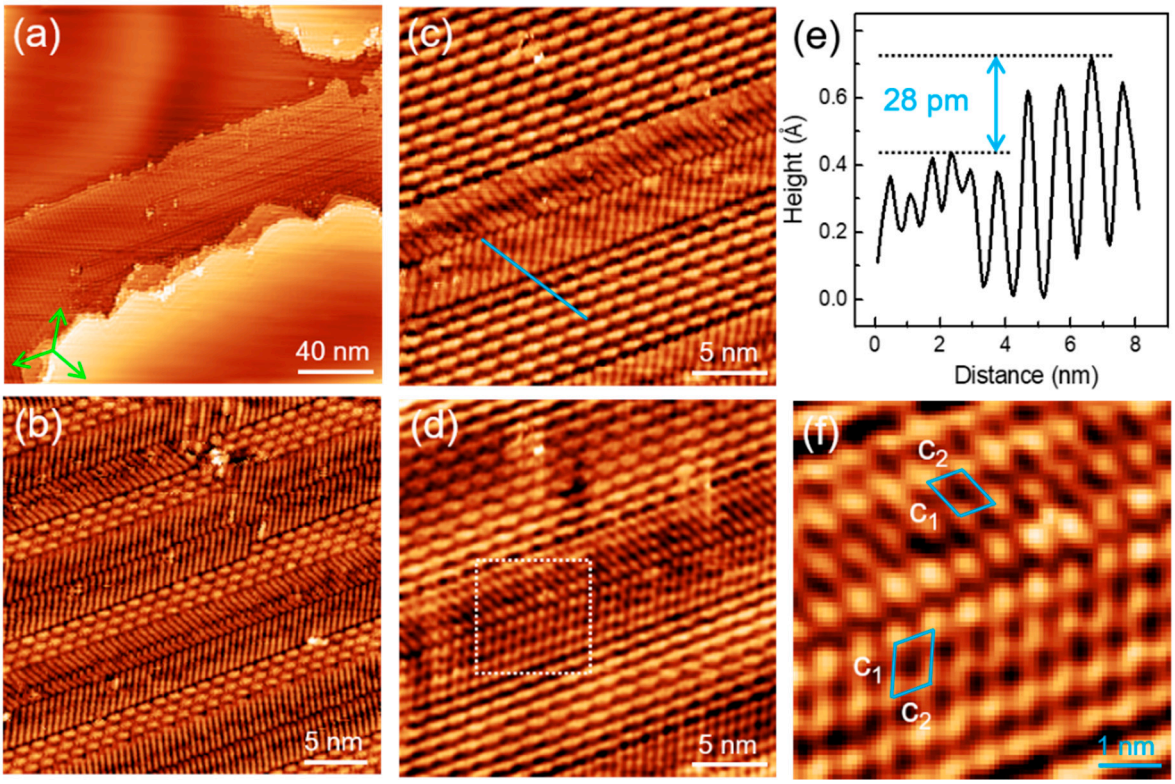

Figure 3. The mixed phase of self-assembled TPB and Cd nanostripes. (**a**) Coexistence of the mixed phase with a domain of 2D self-assembled TPB on the same terrace, −0.5 V, 70 pA. (**b**) Zoom-in images of the mixed phase, −0.1 V, 50 pA. (**c**,**d**) A typical nanostripe of Cd atoms confined by two self-assembled TPB domains. The scanning parameter are 0.1 V, 50 pA (**c**) and 0.01 V, 50 pA (**d**). (**e**) A height profile along the blue line in (**c**), reflecting the height difference between TPB molecules and Cd nanostripes. (**f**) Close-up view of the Cd nanostripes located in the dashed box in (**d**), 0.01 V, 20 pA.

Increasing the molecular coverage to 0.8 mL leads to the formation of pure domains of Cd atomic chains. Figure 4a displays a high-bias STM image of the periodic arrays of Cd nanostrips. Similar to the trenches in the mixed phase, all the Cd stripes run parallel to the lattice directions of Cd(0001) with a periodicity of 5.5 nm. From the close-up view in Figure 4b, it is found that the stripe structures consist of bright ribbons (3.2 nm width) and dim trenches (2.3 nm width). When the sample bias is reduced to 0.16 V (Figure 4c), the striking contrast between the ribbons and trenches is significantly reduced. Instead, the stripe structure reveals a very small height fluctuation. Most importantly, it is observed that the stripe structures are composed of parallel segments of Cd atomic chains, which have two different orientations. They are similar to the trench structures which appeared in the mixed phase. The segments of the atomic chains reveal a length of 2.7 nm, nine times of the lattice constant of Cd(0001). In the atomic-resolution image of Figure 4d, all the Cd dimers exhibit two protrusions, corresponding to two Cd atoms. The inter-chains spacing is 6.0 Å, twice the Cd(0001) lattice constant. Thus, this pure domain of Cd stripes is a commensurate phase with 2 × 2 reconstruction. The appearance of pure stripe domains implies that the long-range (100 nm) mass transport of the substrate atoms takes place on the substrate terraces or step edges. To the best of our knowledge, this is the first observation of massive surface rearrangement and long-range mass transport of substrate atoms occurring on the close-packing metal surface.

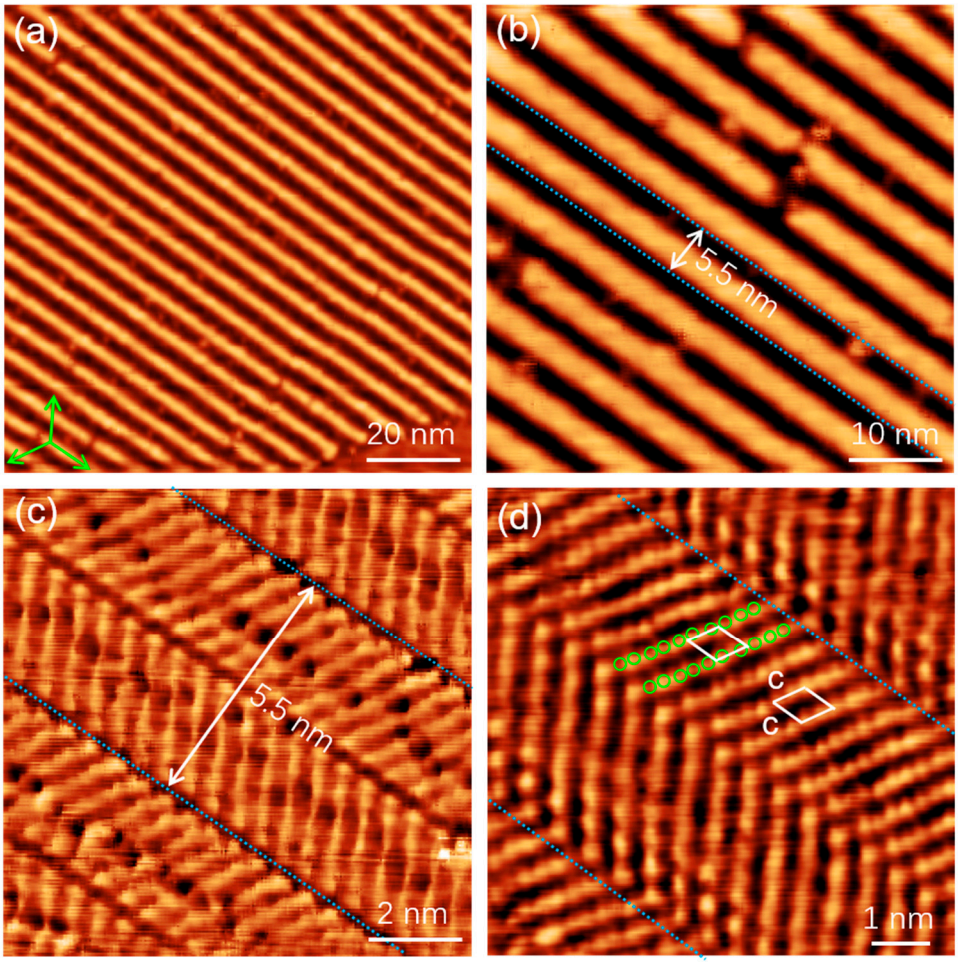

Figure 4. Pure domain of the Cd nanostripes on top of the Cd(0001) surface. (**a**) Periodic arrays of Cd nanostripes of Cd, 3.6 V, 20 pA. (**b**) Zoom-in image of the Cd nanostripes, 3.0 V, 20 pA. (**c**) Parallel segments of Cd atomic chains appeared in the Cd nanostripes, 0.16 V, 20 pA. (**d**) High-resolution STM image of the Cd atom chains with a 2 × 2 reconstruction, 0.1 V, 20 pA.

In order to understand the adsorption-induced substrate reconstruction, we perform density functional theory (DFT) calculations for the TPB adsorption on Cd(0001) (see Supporting Information for details [35–39]). Here, we considered the formation of a single-atom vacancy, where the topmost Cd atom beneath the TPB molecule is removed. As shown in Figure 5, geometry optimization shows strong conformational changes in the TPB molecular structure. The planar TPB molecule exhibits a large downward bending with the central Bi atom closer to the substrate surface than the three benzene rings. Furthermore, one of the three benzene rings is strongly twisted such that it has a larger height than the other two rings, corresponding to the bright protrusion lobes shown in Figures 1d and 2d. The central Bi atom of TPB aligns, in the z direction, with the single-atom vacancy. A close inspection indicates that the distance between the Bi atom and the topmost Cd atoms is 2.34 Å.

The calculated adsorption energy for TPB adsorbed on the single-atom vacancy is 6.28 eV, which is larger than that (5.89 eV) of TPB on the perfect Cd(0001) surface. The large energy difference (0.39 eV) demonstrates that the single-atom vacancy is the preferred adsorption site of the TPB molecules. Thus, the formation mechanism of Cd nanostripes can be attributed to the adsorption-induced singe-atom vacancies driven by the strong TPB-Cd interaction and the subsequent surface diffusion of the Cd adatoms.

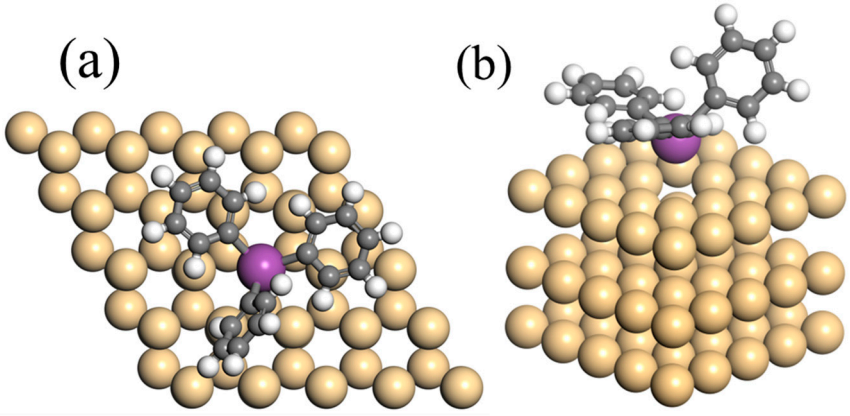

Figure 5. Optimized structure of a TPB molecule attached to a vacancy site on Cd(0001) surface. (**a**) Top view of a TPB molecule sitting on the single-atom pit. (**b**) Three-dimensional sketch of the adsorptional model of TPB on Cd(0001).

4. Conclusions

In summary, TPB molecules adsorbed on the Cd(0001) surface not only lead to the 2D self-assembly of TPB, but also result in the formation of periodic nanostrips of Cd atoms. The 2D self-assembled TPB layer reveals an oblique lattice with $4 \times \sqrt{13}$ reconstruction. In the pure domain of Cd nanostrips, the segments of Cd atomic chains are commensurate with the Cd(0001) substrate with 2×2 reconstruction. In the mixed phase, the Cd atomic chains exhibit only high-order commensuration when confined by the domains of TPB self-assemblies. Such a massive rearrangement of a close-packed meal surface and an unusual long-range mass transport can be attributed to the complex molecule–substrate interactions.

Supplementary Materials: The following supporting information can be downloaded at: https://www.mdpi.com/article/10.3390/coatings13020394/s1, Figure S1: (a) High-bias STM image of the mixed phase made of Cd nanostripes and TPB layer, U = 3.5 V. (b) Height profile line along the dotted line in (a).

Author Contributions: Conceptualization, M.B.; methodology, M.B.; software, Z.L.; validation, M.B.; formal analysis, M.T.; investigation, M.B., X.Y. and M.S.; resources, J.W.; data curation, M.B., M.S. and J.W.; writing—original draft preparation, M.B.; writing—review and editing, M.T., K.S., Z.L. and J.W.; visualization, M.B. and K.S.; supervision, J.W.; project administration, J.W.; funding acquisition, Y.Z. and J.W. All authors have read and agreed to the published version of the manuscript.

Funding: This research was supported by the National Natural Science Foundation of China (Grant Nos. 11874304, 11574253).

Conflicts of Interest: We have no conflict of interest.

References

1. Goronzy, D.P.; Ebrahimi, M.; Rosei, F.; Arramel; Fang, Y.; De Feyter, S.; Tait, S.L.; Wang, C.; Beton, P.H.; Wee, A.T.S.; et al. Supramolecular Assemblies on Surfaces: Nanopatterning, Functionality, and Reactivity. *ACS Nano* **2018**, *12*, 7445–7481. [CrossRef] [PubMed]
2. Gimzewski, J.K.; Modesti, S.; Schlittler, R.R. Cooperative Self-Assembly of Au Atoms and C60 on Au(110) Surfaces. *Phys. Rev. Lett.* **1994**, *72*, 1036–1039. [CrossRef] [PubMed]
3. Rosei, F.; Schunack, M.; Naitoh, Y.; Jiang, P.; Gourdon, A.; Laegsgaard, E.; Stensgaard, I.; Joachim, C.; Besenbacher, F. Properties of Large Organic Molecules on Metal Surfaces. *Prog. Surf. Sci.* **2003**, *71*, 95–146. [CrossRef]
4. Xu, Z.; Wu, Q.; Zhang, Y.; Hou, S.; Wang, Y. Ordered Patterns of Copper Phthalocyanine Nanoflowers Grown around Fe Islands on Au(111). *J. Clust. Sci.* **2022**, *33*, 2393–2397. [CrossRef]
5. Klappenberger, F. Two-Dimensional Functional Molecular Nanoarchitectures—Complementary Investigations with Scanning Tunneling Microscopy and X-ray Spectroscopy. *Prog. Surf. Sci.* **2014**, *89*, 1–55. [CrossRef]
6. Weckesser, J.; Cepek, C.; Fasel, R.; Barth, J.V.; Baumberger, F.; Greber, T.; Kern, K. Binding and Ordering of C60 on Pd(110): Investigations at the Local and Mesoscopic Scale. *J. Chem. Phys.* **2001**, *115*, 9001–9009. [CrossRef]
7. Hsu, C.L.; Pai, W.W. Aperiodic Incommensurate Phase of a C-60 Monolayer on Ag(100). *Phys. Rev. B* **2003**, *68*, 245414. [CrossRef]

8. Pai, W.; Hsu, C.L. Ordering of an Incommensurate Molecular Layer with Adsorbate-Induced Reconstruction: C60/Ag(100). *Phys. Rev. B-Condens. Matter Mater. Phys.* **2003**, *68*, 121403. [CrossRef]
9. Hinterstein, M.; Torrelles, X.; Felici, R.; Rius, J.; Huang, M.; Fabris, S.; Fuess, H.; Pedio, M. Looking underneath Fullerenes on Au(110): Formation of Dimples in the Substrate. *Phys. Rev. B* **2008**, *77*, 153412. [CrossRef]
10. Rosei, F.; Schunack, M.; Jiang, P.; Gourdon, A.; Lægsgaard, E.; Stensgaard, I.; Joachim, C.; Besenbacher, F. Organic Molecules Acting as Templates on Metal Surfaces. *Science* **2002**, *296*, 328–331. [CrossRef]
11. Otero, R.; Rosei, F.; Naitoh, Y.; Jiang, P.; Thostrup, P.; Gourdon, A.; Laegsgaard, E.; Stensgaard, I.; Joachim, C.; Besenbacher, F. Nanostructuring Cu Surfaces Using Custom-Designed Molecular Molds. *Nano Lett.* **2004**, *4*, 75–78. [CrossRef]
12. Schunack, M.; Rosei, F.; Naitoh, Y.; Jiang, P.; Gourdon, A.; Lægsgaard, E.; Stensgaard, I.; Joachim, C.; Besenbacher, F. Adsorption Behavior of Lander Molecules on Cu(110) Studied by Scanning Tunneling Microscopy. *J. Chem. Phys.* **2002**, *117*, 6259–6265. [CrossRef]
13. Schunack, M.; Petersen, L.; Kuhnle, A.; Laegsgaard, E.; Stensgaard, I.; Johannsen, I.; Besenbacher, F. Anchoring of Organic Molecules to a Metal Surface: HtBDC on Cu(110). *Phys. Rev. Lett.* **2001**, *86*, 456–459. [CrossRef]
14. Witte, G.; Hanel, K.; Busse, C.; Birkner, A.; Woell, C. Molecules Coining Patterns into a Metal: The Hard Core of Soft Matter. *Chem. Mater.* **2007**, *19*, 4228–4233. [CrossRef]
15. Tseng, T.C.; Urban, C.; Wang, Y.; Otero, R.; Tait, S.L.; Alcamí, M.; Écija, D.; Trelka, M.; Gallego, J.M.; Lin, N.; et al. Charge-Transfer-Induced Structural Rearrangements at Both Sides of Organic/Metal Interfaces. *Nat. Chem.* **2010**, *2*, 374–379. [CrossRef]
16. Böhringer, M.; Berndt, R.; Schneider, W.D. Transition from Three-Dimensional to Two-Dimensional Faceting of Ag(110) Induced by Cu-Phthalocyanine. *Phys. Rev. B-Condens. Matter Mater. Phys.* **1997**, *55*, 1384–1387. [CrossRef]
17. Gross, L.; Moresco, F.; Alemani, M.; Tang, H.; Gourdon, A.; Joachim, C.; Rieder, K.H. Lander on Cu(211)—Selective Adsorption and Surface Restructuring by a Molecular Wire. *Chem. Phys. Lett.* **2003**, *371*, 750–756. [CrossRef]
18. Kuhnle, A.; Molina, L.M.; Linderoth, T.R.; Hammer, B.; Besenbacher, F. Growth of Unidirectional Molecular Rows of Cysteine on Au(110)-(1x2) Driven by Adsorbate-Induced Surface Rearrangements. *Phys. Rev. Lett.* **2004**, *93*, 086101. [CrossRef]
19. Gross, L.; Rieder, K.H.; Moresco, F.; Stojkovic, S.M.; Gourdon, A.; Joachim, C. Trapping and Moving Metal Atoms with a Six-Leg Molecule. *Nat. Mater.* **2005**, *4*, 892–895. [CrossRef]
20. Trevethan, T.; Such, B.; Glatzel, T.; Kawai, S.; Shluger, A.L.; Meyer, E.; de Mendoza, P.; Echavarren, A.M. Organic Molecules Reconstruct Nanostructures on Ionic Surfaces. *Small* **2011**, *7*, 1264–1270. [CrossRef]
21. Zhang, J.; Zhao, S.X.; Yuan, B.K.; Deng, K.; Sun, B.Y.; Qiu, X.H. Monolayered Adatom Aggregation Induced by Metallofullerene Molecules on Cu(100). *Surf. Sci.* **2012**, *606*, 78–82. [CrossRef]
22. Dong, L.; Sun, Q.; Zhang, C.; Li, Z.W.; Sheng, K.; Kong, H.H.; Tan, Q.G.; Pan, Y.X.; Hu, A.G.; Xu, W. A Self-Assembled Molecular Nanostructure for Trapping the Native Adatoms on Cu(110). *Chem. Commun.* **2013**, *49*, 1735–1737. [CrossRef] [PubMed]
23. Shi, Y.; Choi, B.Y.; Salmeron, M. Water Chains Guide the Growth of Monoatomic Copper Wires on Cu(110). *J. Phys. Chem. C* **2013**, *117*, 17119–17122. [CrossRef]
24. Abadía, M.; González-Moreno, R.; Sarasola, A.; Otero-Irurueta, G.; Verdini, A.; Floreano, L.; Garcia-Lekue, A.; Rogero, C. Massive Surface Reshaping Mediated by Metal–Organic Complexes. *J. Phys. Chem. C* **2014**, *118*, 29704–29712. [CrossRef]
25. Kalashnyk, N.; Rochford, L.A.; Li, D.Z.; Smogunov, A.; Dappe, Y.J.; Jones, T.S.; Guillemot, L. Unraveling Giant Cu(110) Surface Restructuring Induced by a Non-Planar Phthalocyanine. *Nano Res.* **2018**, *11*, 2605–2611. [CrossRef]
26. Paßens, M.; Karthäuser, S. Interfacial and Intermolecular Interactions Determining the Rotational Orientation of C60 Adsorbed on Au(111). Surf. *Sci.* **2015**, *642*, 11–15. [CrossRef]
27. Pai, W.W.; Hsu, C.L.; Lin, M.C.; Lin, K.C.; Tang, T.B. Structural Relaxation of Adlayers in the Presence of Adsorbate-Induced Reconstruction: C60/Cu(111). *Phys. Rev. B-Condens. Matter Mater. Phys.* **2004**, *69*, 125405. [CrossRef]
28. Li, H.I.; Pussi, K.; Hanna, K.J.; Wang, L.L.; Johnson, D.D.; Cheng, H.P.; Shin, H.; Curtarolo, S.; Moritz, W.; Smerdon, J.A.; et al. Surface Geometry of C60 on Ag(111). *Phys. Rev. Lett.* **2009**, *103*, 056101. [CrossRef]
29. Stöhr, M.; Gabriel, M.; Möller, R. Investigation of the Growth of PTCDA on Cu(1 1 0): An STM Study. *Surf. Sci.* **2002**, *507–510*, 330–334. [CrossRef]
30. Murray, P.; Pedersen, M.; Lægsgaard, E.; Stensgaard, I.; Besenbacher, F. Growth of on Cu(110) and Ni(110) Surfaces:-Induced Interfacial Roughening. *Phys. Rev. B-Condens. Matter Mater. Phys.* **1997**, *55*, 9360–9363. [CrossRef]
31. Jones, P.G.; Blaschette, A.; Henschel, D.; Weitze, A. Redetermination of the Crystal Structure of triphenylbismuth, (C6H5)3Bi. *Zeitschrift Fur Krist.* **1995**, *210*, 377–378. [CrossRef]
32. Wang, Z.F.; Liu, Z.; Liu, F. Organic Topological Insulators in Organometallic Lattices. *Nat. Commun.* **2013**, *4*, 1–5. [CrossRef]
33. Wang, R.S.; Cheng, J.; Wu, X.L.; Yang, H.; Chen, X.J.; Gao, Y.; Huang, Z.B. Superconductivity at 3.5 K and/or 7.2 K in Potassium-Doped Triphenylbismuth. *J. Chem. Phys.* **2018**, *149*, 144502. [CrossRef]
34. Wang, R.S.; Yang, H.; Cheng, J.; Wu, X.L.; Fu, M.A.; Chen, X.J.; Gao, Y.; Huang, Z.B. Discovery of Superconductivity in Potassium-Doped Tri-p-Tolylbismuthine. *J. Phys. Chem. C* **2019**, *123*, 19105–19111. [CrossRef]
35. Vande, V.J.; Krack, M.; Mohamed, F.; Parrinello, M.; Chassaing, T.; Hutter, J. QUICKSTEP: Fast and accurate density functional calculations using a mixed Gaussian and plane waves approach. *Comput. Phys. Commun.* **2005**, *167*, 103–128. [CrossRef]
36. Perdew, J.; Burke, P.K.; Ernzerhof, M. Generalized Gradient Approximation Made Simple. *Phys. Rev. Lett.* **1996**, *77*, 3865. [CrossRef] [PubMed]
37. Monkhorst, H.J.; Pack, J.D. Special points for Brilloofn-zone integrations. *Phys. Rev. B* **1976**, *13*, 5188–5192. [CrossRef]

38. Bucko, T.; Hafner, J.; Lebegue, S.; Angy'an, J.G. Improved Description of the Structure of Molecular and Layered Crystals: Ab Initio DFT Calculations with van der Waals Corrections. *J. Phys. Chem. A* **2010**, *114*, 11814–11824. [CrossRef]
39. Lu, T.; Chen, F. Multiwfn: A Multifunctional Wavefunction Analyzer. *J. Comput. Chem.* **2012**, *33*, 580–592. [CrossRef]